IEEE Access
Multidisciplinary ⋮ Rapid Review ⋮ Open Access Journal

Received 13 October 2023, accepted 19 October 2023, date of publication 27 October 2023, date of current version 7 November 2023.

Digital Object Identifier 10.1109/ACCESS.2023.3328177

RESEARCH ARTICLE

Development of a Simulation and Control Platform for the China ADS Based on a Thermal Coupling Method

TAO ZHANG[1], BO SHI[1], ZHIJIANG WU[1], TIANJIAO ZHANG[1], YAN WANG[1], AND WEI GUO[1,2]

[1]China Nuclear Power Technology Research Institute, Shenzhen, Guangdong 518031, China
[2]School of Power and Energy Engineering, Harbin Engineering University, Harbin, Heilongjiang 150006, China

Corresponding author: Bo Shi (shibo.cgn@foxmail.com)

This work was supported by Project of Shenzhen Key Laboratory of Nuclear Radiation Detector and Electronics System under Grant ZDSYS20220606100804011.

ABSTRACT Accelerator driven subcritical reactors have attracted much attention in recent years for their ability to generate energy and transform radioactive waste in a cleaner and safer manner. As an important part of accelerator driven subcritical system (ADS), control system is directly related to the stable and safe operation of the system. Therefore, it is necessary to build a high-precision control system simulation platform that is easy to design and verify. In this paper, a simulation platform coupling Simulink and Locust is developed for the control system design of ADS in China. Based on an explicit thermal coupling strategy (TCS) of interface heat flux and wall temperature, the entire closed-loop system model is established. The simulation platform is divided into two parts according to the coolant type: the first part with lead bismuth eutectic is composed of the shell side of the interface heat exchanger (IHX), reactor, and main pump; the second part with water include the tube side of IHX, air cooler, feedwater pump, and flow network. To verify the effectiveness of the TCS method, the thermohydraulics parameters of once-through steam generator (OTSG) calculated by the coupled model were compared with those calculated by single Locust model under steady and transient conditions.The results show that the two models have good consistency. The coupled platform is able to successfully simulate dynamic processes under different conditions. In addition, simulation verification is carried out under the step change of 10% FP to study its control characteristics. The results show that the control effect of the coupled platform is slightly better than that of single Locust. The control system has a good ability to adjust the ADS system, and extends the functions of traditional Locust without modifying the Locust source code. While ensuring the accuracy of the model, it increases the flexibility of modeling and improves the modeling efficiency, which can provide an important reference for further engineering applications.

INDEX TERMS Accelerator driven subcritical systems, lumped parameter model, moving nodal model, control strategy, simulation.

I. INTRODUCTION

Accelerator driven subcritical nuclear reactor has been attention widely, which is used to generate energy and transmute spent fuel in a clean and safe approach [1], [2]. In recent years, various accelerator driven subcritical system (ADS) concepts have been proposed, including ''PDS-XADS'' project and ''FUTURES'' project proposed in the 5th Framework Programme (FP), ''XT-ADS'' project and ''EFIT'' project followed in the 6th FP [3], [4], [5], and ''MYRRHA'' project developed by SC-CE in the European Union [6]. Furthermore, various design and technology development activities are also being conducted in the US, Russia, Japan, and Korea [7], 8. Meanwhile, lead-bismuth Eutectic (LBE) cooled ADS systems have been designed in China, namely the ''CLEA'' series. China LEAd-based Reacto (CLEAR),

The associate editor coordinating the review of this manuscript and approving it for publication was Guillermo Valencia-Palomo.

aiming to transmute nuclear waste has been launched by Chinese Academy of Sciences (CAS) in 2011. A 10MW research reactor CLEAR-1 will be designed and built [9]. China Initiative Accelerator Driven System, an LBE cooled subcritical reactor, was also approved by the National Development and Reform Commission [10].

In the China ADS system, neutrons are produced by utilizing highly intensified and high-energy protons to hi heavy metal spallation for maintaining chain fission reaction. The thermal power in the core is carried out by the LBE coolant, is transferred to the pressurize water in the interface heat exchanger (IHX), and is cooled by an air cooler for an effective rejection to the environment as a final heat sink [11]. Because of the system composition and operating characteristic, the China ADS is different from the traditional light water reactors (LWRs), especially the actual ADS reactor has not been built to design and verify control system. Simulation is an effective approach to study dynamic characteristics and design control system. In recent years, two methods for modeling and simulation have been adopted widely. The lumped parameter method was used to develop the ADS models by Yan et al. [12] and Yin et al. [13]. This method is convenient to establish a subcritical reactor model with LBE coolant. However, a lot of simplification and assumptions reduce the accuracy of the thermal hydraulic (TH) model. Nodal models developed by commercial TH codes or modified TH codes, such as Locust and Theatre, have sufficient accuracy for safety assessment, thermal hydraulic design, and operator training [14], [15], [16]. However, these codes cannot be directly used to design model-based controllers, nor can they be used to efficiently simulate complex control logic.

Because of the difficulty in model development and control system design in the ADS system by single simulation code, the couping method has been developed to expand the functions of the single software. Lin et al. has accomplished control systems verification and validation of LWRs based on the coupling method between Locust and Simulink. In his work, control and protection logic was simulated by Simulink, and the be-estimated plant model was established by Locust [17]. Toti et al. developed a multi-scale modeling method using coupled Locust-3D and CFD code for computing heat transfer phenomena and analysis of a total loss flow transient of MYRRHA based on the hydraulic coupling and thermal coupling method. These coupling methods expand the ability of modeling and simulation of the ADS [18]. Li et al. Combined with the lumped parameter method and the point reactor kinetics method, describe the dynamic characteristics of the ADS power control was established physical model, and the quantum evolutionary algorithm (QEA) was used to get the appropriate a set of parameters in PID controller. Finally, the performance of the optimization method is verified in a predefined control scenario [19].

In view of the fact that the latest ADS in China is under construction and there is no practical engineering application reference for the design and verification of the control system, this paper makes the following improvements to the Locust thermal hydraulics software independently developed by China General Nuclear Power Group on the basis of fully combining the above research methods, in order to provide reference and guidance for the engineering design and verification of new reactors such as LBE.

1. A thermal coupling method is proposed to develop the ADS model without modifying the Locust source code, and the data exchange between the Locust simulation software and Simulink simulation software in ADS system is implemented.

2. The primary loop model is established by Simulink, and the secondary loop model is established by Locust to realize the thermal coupling data transmission of the platform. The feasibility of the thermal coupling platform is verified by comparing the errors of the primary loop model and the secondary loop model established by the thermal coupling platform and single Locust platform.

3. Based on the same control parameters, the control strategies of the thermal coupling platform and the single Locust platform are compared and analyzed under steady-state and transient conditions to verify the accuracy of the coupled platform.

II. THE CHINA ADS SYSTEM DESCRIPTION

The China ADS system, a conceptual design of a subcritical reactor, is a liquid lead-bismuth cooled fast reactor with the semi-pool type arrangement mode, as shown in Fig.1. The main equipment of the China ADS includes the accelerator, the spallation target, the subcritical core, IHX, the air cooler, and the feed water pump.

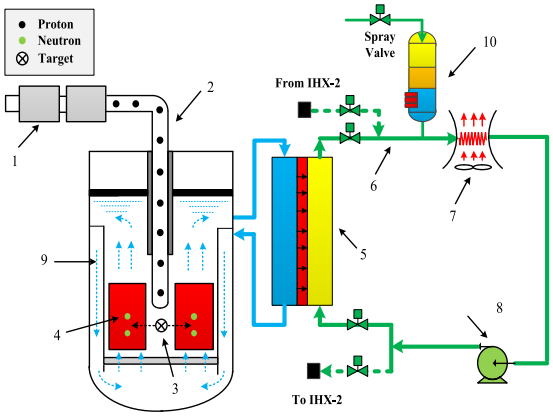

FIGURE 1. Schematic structure of the china ADS system.

In the primary loop, protons beam from the accelerator are introduced into the target and hit the lead target, and then neutrons are supplied to the core and be used to maintain fission reaction. The thermal power is carried out by the LBE coolant. Then, the heat is transferred to the pressurized water through the wall of tubes in IHXs. The water is cooled by the air in the air cooler to effective rejection of thermal power to

TABLE 1. Main design data of the china ADS system.

Parameters	Unit	Value
Core power	MW	10
Core inlet temperature(100%FP)	K	553.15
Core outlet temperature(100%FP)	K	653.15
Primary coolant	-	LBE
Coolant mass flow rate in the core	kg/s	533
Secondary coolant	-	Water
Secondary side coolant pressure	MPa	8
Secondary side inlet temperature	K	498.15
Secondary side outlet temperature	K	533.15
Heat sink	-	Air cooler
Air cooler secondary side inlet temperature	K	303.15

the environment as a final heat sink. The main design data are summarized in Table 1 [20].

Since the design process of this China ADS system is still going on, the present work reveals the preliminary results. The future work will partly re-model the equipment of the system, such as IHXs and air coolers.

III. THERMAL COUPLING METHOD

The model of the China ADS is divided to two parts according to the coolant type in different closed-loop system as shown in Fig.2. The primary model with LBE coolant is composed by the shell side of interface heat exchanger, core, upper plenum and down plenum; the secondary model with water coolant is composed by the tube side of IHX, air cooler, feedwater pump and flow network. The former is developed by Simulink and the latter is developed by Locust.

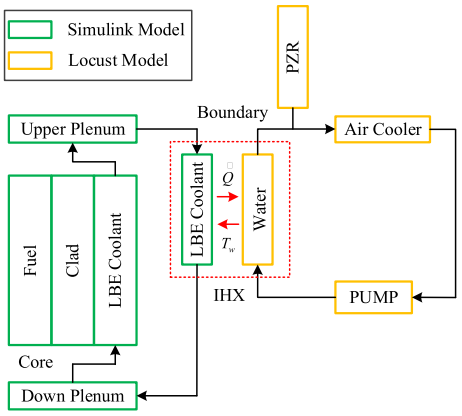

FIGURE 2. Modeling and coupling method of the china ADS system.

The data exchange method at thermal coupling interfaces is shown in Fig.3. The wall temperature and heat flux are selected as the parameters for implementing coupled computing between Locust model and Simulink model. In the coupled calculation process, Locust computes the wall temperature $T_{w,i}$ of each node i, which is sent to node i of the Simulink as the interface parameter. In turn, for each interface node i Simulink computes the average heat flux q_i according

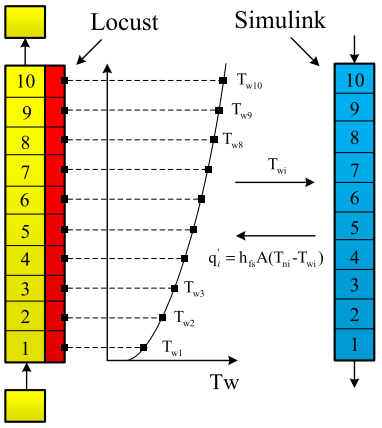

FIGURE 3. Data exchange method at thermal coupling interfaces.

to the wall temperature $T_{w,i}$, and sends the average heat flux to Locust at each node as boundary parameter.

IV. ADS WHOLE SYSTEM SIMULATION PLATFORM

A. THE PRIMARY SYSTEM MODEL

In this part, lumped parameter models of the primary loop system, composed by core and the shell side of IHX are given based on the fundamental conservation laws of mass and energy. The models are developed by Simulink.

1) CORE MODEL

a: NEUTRONIC KINETICS MODEL

The point kinetics equations with six groups delayed neutron for ADS subcritical core with an external neutron source is applied to perform the neutronics module calculation [21], the equations are given by:

$$\begin{cases} \dfrac{dn(t)}{dt} = \left(\dfrac{K_{eff}-1}{K_{eff}} + \rho(t) - \beta\right)\dfrac{n(t)}{\Lambda} + \sum_{i=1}^{6}\lambda_i c_i(t) + q(t) \\ \dfrac{dc_i(t)}{dt} = \dfrac{\beta_i}{\Lambda}n(t) - \lambda_i c_i(t) \qquad i = 1, 2, \ldots, 6 \end{cases} \tag{1}$$

where $n(t)$ is neutron density at time$t$, $\rho(t)$ is the total reactivity, β is the effective delayed neutron, Λ is the prompt neutron lifetime, λ_i is the decay constant for the delayed neutron precursors group i, C_i is the number of delayed neutron precursors in group i.

The reactivity feedback coefficients of the point kinetics equations are expressed as the function of the average temperatures of fuel and LBE coolant. As a result, the total reactivity $\rho(t)$can be represented as:

$$\rho(t) = \rho_0 + \rho_p(t) + \alpha_f(T_f - T_{f0}) + \alpha_c(T_c - T_{c0}) \tag{2}$$

where ρ_0 is the initial reactivity, $\rho_p(t)$ is the proton beam introduced reactivity. T_{f0} and T_{c0} denote the reference temperatures of fuel and LBE coolant, T_f and T_c denote the temperatures of fuel and LBE coolant, α_f and α_c denote the reactivity feedback coefficients of fuel and LBE coolant.

b: THERMAL-HYDRAULICS MODEL

The Mann's model was used in this study to calculate the fuel temperature and coolant temperature variations during transient process. As shown in Fig.3(a), LBE coolant in two coolant nodes are well mixed, so the outlet temperatures of each node equal to the average temperatures of these two coolant nodes [22]. The heat transfer equations of the with section along the axial direction are expressed as:

$$\begin{cases} M_{f,i}C_{f,i}\dfrac{dT_{f,i}(t)}{dt} \\ = P_i(t) - U_{fc,i}(T_{f,i}(t) - T_{c,i}(t)); \quad i = 1, 2 \\ M_{L,1}C_{L,1}\dfrac{dT_{c,1}(t)}{dt} \\ = U_{fc,1}(T_f(t) - T_{c,1}(t)) - \omega_{L,1}C_{L,1}(T_{c,1}(t) - T_{c,in}(t)) \\ M_{L,2}C_{L,2}\dfrac{dT_{c,2}(t)}{dt} \\ = U_{fc,2}(T_f(t) - T_{c,2}(t)) - \omega_{L,2}C_{L,2}(T_{c,2}(t) - T_{c,1}(t)) \end{cases} \tag{3}$$

where $T_{f,i}$, $T_{c,1}$, $T_{c,2}$ and $T_{c,in}$ are fuel average temperature, temperatures of two coolant nodes and inlet coolant temperature; U_{fc} is transfer coefficient between the fuel and coolant

Fuel rod arrangement scheme is shown in Fig.3 (b). The total heat transfer coefficient from fuel to LBE coolant is expressed as:

$$U_{fc} = \frac{1}{\frac{1}{4\pi L_f \lambda_f} + \frac{1}{2\pi r_f L_f h_g} + \frac{\ln(r_{co}/r_{ci})}{2\pi L_f \lambda_c} + \frac{1}{2\pi r_{co} L_f h_{c,LB}}} \tag{4}$$

where L_f denotes the fuel rod length, r_{co} and r_{ci} denote the inner and outer radius of fuel cladding, λ_f is the fuel thermal conductivity, λ_c is the fuel thermal conductivity, h_g is the overall gap conductance between fuel and cladding, A_c is the total heat transfer area of cladding, and $h_{c,LBE}$ is the convective heat transfer coefficient between the cladding and the LBE coolant according to the Subbotln/Ushakov correlation [23].

The heat transfer mechanism of LBE metal is quite different from that of water and other fluids. A lot of heat transfer correlations have been presented. In most of the cases, Subbotin/Ushakov correlation calculates the average heat transfer coefficient and the biggest validity range of fuel rods pitch diameter ratio (P/D). All results presented in this part are calculated by this correlation.

Subbotin/Ushakov correlation:

$$Nu = 7.55\frac{P}{D} - 20\left(\frac{P}{D}\right)^{-13} + \frac{3.67}{90\left(\frac{P}{D}\right)^2} Pe^{\left(0.56+0.19\frac{P}{D}\right)} \tag{5}$$

Validity range: $1 \le Pe \le 4000$, $1.2 \le P \le 2.0$.

where Nu is the Nusslet number, Pe is the Peclet number, P is the pitch of fuel rods, and D is the diameter of fuel rod.

2) THE SHELL SIDE MODEL OF IHX

The IHX is of the helical tubes, single pass and counter current type. LBE coolant flows in the shell side with temperature decrease. Meanwhile, the water flows in the tube side with temperature increase. Assuming heat exchange between IHX and surroundings is neglected. Because of not considering pressure drop, the model used the mass and energy equation is satisfied to describe the dynamic characteristic of IHX [24]. The model is divided to 10 nodes. The mass and energy equations of each node are described as:

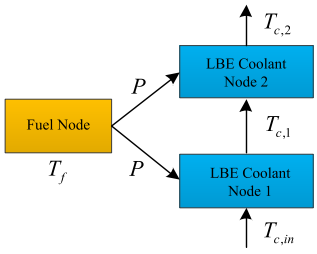

(a) Heat transfer between fuel and coolant

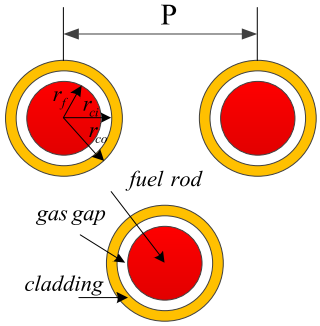

(b) Fuel rod arrangement scheme

FIGURE 4. Schematic diagrams of the core model.

$$\begin{cases} V_{sc,1}\dfrac{d(d_{sc,1})}{dt} = W_{sc,1} - W_{sc,in} \\ V_{sc,i}\dfrac{d(d_{sc,i})}{dt} = W_{sc,i} - W_{sc,i-1} \quad i = 2 \sim 9 \\ V_{sc,10}\dfrac{d(d_{sc,10})}{dt} = W_{sc,out} - W_{sc,10} \\ \mu_{sc,1}\dfrac{d(T_{sc,1})}{dt} = C_{sc,1}W_{sc,in}(T_{sc,in} - T_{sc,1}) \\ -h_{fs,i}A_1(T_{m,1} - T_{w,1}) \\ \mu_{sc,i}\dfrac{d(T_{sc,i})}{dt} = C_{sc,i}W_{sc,i-1}(T_{sc,i-1} - T_{sc,i}) \\ -h_{fs,i}A_i(T_{m,i} - T_{w,i}) \quad i = 2 \sim 9 \\ \mu_{sc,10}\dfrac{d(T_{sc,10})}{dt} = C_{sc,10}W_{sc,10}(T_{sc,9} - T_{sc,out}) \\ -h_{fs,10}A_{10}(T_{m,10} - T_{w,10}) \end{cases} \tag{6}$$

The air cooler is special equipment with finned tubes, in which water of tube side flowing in horizontal direction is cooled by air of shell side flowing in vertical direction. In the tube side, heat transfer tubes are equivalent to single tube and are simulated by 317P. In the shell side, airflow is modeled by 603P with the inlet temperature imposed in TDV601 and the inlet mass flow imposed in TDJ602. The heat structure is simulated by 701ht using cylindrical geometry. The heat transfer area of 603P node-3 is equal to the total area of 317P.

TABLE 2. Thermo-physical properties of LBE.

Property	Calculation formula
Fuel specific heat capacity	$C_f = \frac{214.65\times C_{UO_2} + 55.56\times C_{PuO_2}}{270.21}$ C_{UO_2} -UO_2 spcific heat capacity C_{PuO_2} -PuO_2 spcific heat capacity
Fuel thermal conductivity	$\lambda_f = \frac{1}{0.042+T\times 2.71\times 10^{-4}} + T^3\times 6.9\times 10^{-11}$
Clad thermal conductivity	$\lambda_c = 15.4767 + T\times 3.448\times 10^{-3}$
Coolant density	$\rho_{LB} = 11112 - 1.375T$
Coolant specific heat capacity	146.5
Coolant thermal conductivity	$\lambda_c = 3.9021 + T\times 0.0123$
Gas gap heat exchange coefficient	$h_g = \frac{3.623\times 10^{-3}\times T_g^{0.66}}{R_g}$, T_g -gas gap temperature R_g -gas gap thickness

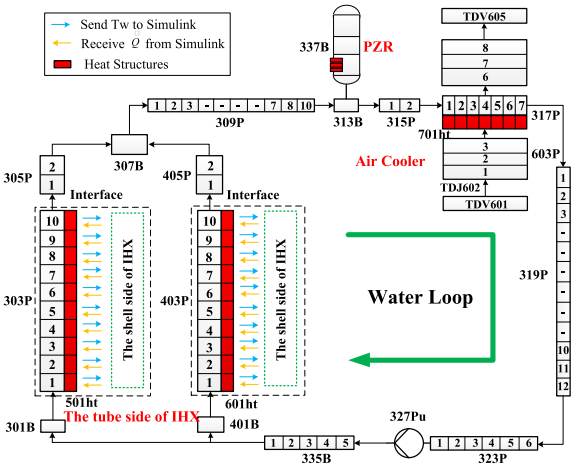

FIGURE 5. The Locust nodalization model of the secondary loop.

B. THE CONTROL SYSTEM MODEL

Keeping the LBE inlet temperature of core close to the reference value is the main purpose of the control strategy. There are three sets of control systems: the power control system, the feedwater control system and the fan blowing rate control system. The aim of the power control strategy is to keep the power following the requirement by changing the proton beam manually. The schematic diagram of feedwater control and fan blowing rate control system is illustrated in Fig.6.

For the choice of control scheme, we have found some novel control schemes that may be suitable for this platform, including: Adaptive control, active disturbance rejection control, etc., [25], [26], and [27]. However, since the nuclear power control system is particularly important for the consideration of safety, the above new control algorithms are still in the theoretical research stage in our new reactor, and there are no practical engineering application cases of advanced control algorithms in previous nuclear power control systems.

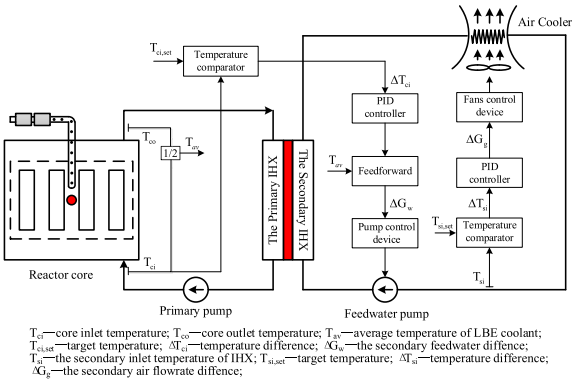

T_{ci}—core inlet temperature; T_{co}—core outlet temperature; T_{av}—average temperature of LBE coolant; $T_{ci,set}$—target temperature; ΔT_{ci}—temperature difference; ΔG_w—the secondary feedwater diffence; T_{si}—the secondary inlet temperature of IHX; $T_{si,set}$—target temperature; ΔT_{si}—temperature difference; ΔG_g—the secondary air flowrate diffence;

FIGURE 6. Schematic diagram of control strategy.

Considering that the main purpose of this paper is to verify that compared with the single Locust platform, the coupled platform can not only ensure the accuracy of the ADS model, but also increase the modeling flexibility and modeling efficiency, the conventional PID controller, which is very mature in the nuclear power control system, is used in this paper for the control system design.

C. THE FEEDWATER CONTROL SYSTEM

The water flowrate control system is to keep the core inlet temperature at 553.15K by controlling the speed of feedwater pump for preventing the LBE temperature of primary loop lower than its melting point.

A single feedback-feedfoward control method is adopted for this control system. The feedback block is PI controller, while the feedforward block consists of a function generator relating the required water flowrate G_w to the average temperature T_{av} of LBE coolant for short adjustment time. The speed of feedwater pump is changed according to the feedwater requirement signal, which is calculated by the PI output signal and feedforward output signal.

The feedwater flowrate is calculated as follows:

$$G_w = K_p \Delta T_{ci} + K_i \int_0^t \Delta T_{ci} dt + F(T_{av}) \tag{7}$$

where $\Delta T_{ci} = T_{ci,set} - T_{ci}$ is the error signal, K_p is the proportional gain, K_i is the integral gain, and $F(T_{av})$ is the feedforward function, which relates the feedwater flowrate to the average temperature of core.

D. THE FAN BLOWING RATE CONTROL SYSTEM

The fan blowing rate control system is used to keep the inlet temperature of the secondary side of IHX at the reference value for optimization of the feedwater control. A feedback control method is adopted for this control system. The feedback block is PI controller. The deviation of the inlet temperature of IHX and the reference value is input signal of PI controller. Then the fans blowing rate is changed according to the signal which is calculated by the PI output signal.

V. VALIDATION OF THE COUPLING METHOD

The choice of boundary interface affects to the stability and accuracy of coupling. However, the thermal coupling is rarely studied by other researchers. In this part, the model of IHX is used to test and verify the correctness of the thermal coupling method in steady state and transient conditions through comparing the results calculated by single Locust. The models of LBE side and water side are named 323P and 303P respectively. The initial conditions of the IHX under 100%FP are shown in Table 1.

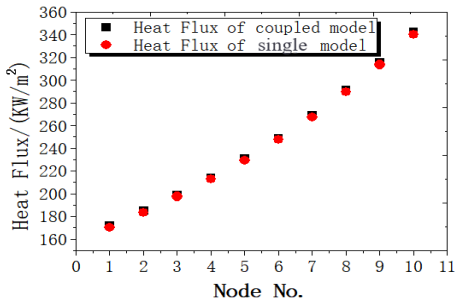

(a) The heat flux of each node

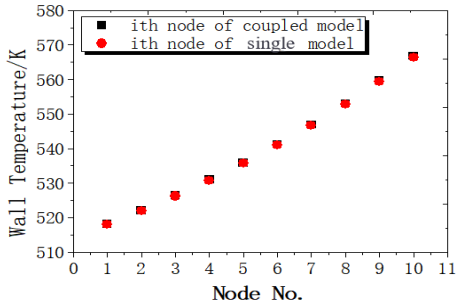

(b) The wall temperature of each node

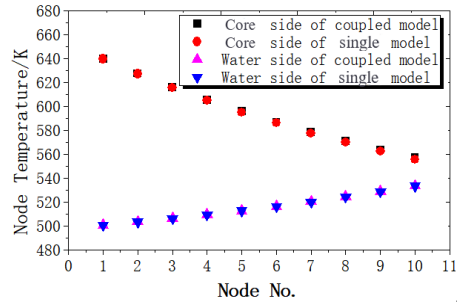

(c) Average temperature of each node

FIGURE 7. Comparison of steady-state results between the two codes.

A. THE VALIDATION OF STEADY-STATE CONDITION

Fig.7 (a) and (b) show the comparison of the wall temperature and heat flux of the IHX between the coupling code and single Locust code. Fig.7 (c) shows the fluid temperature variation along the heat transfer tube of the IHX. The secondary water temperature increases when water flows upward in the tube side. The primary LBE flows downward from node ten to the node one in the shell side, and the temperature decreases when it flows down.

Table 3 and Table 4 show the comparison of IHX wall temperature, heat flux and temperature change of each node under steady-state condition. It can be seen that the numerical deviation calculated by the coupled model and the single Locust model is very small, which indicates that the coupled model has a good fit.

TABLE 3. The comparison of the wall temperature and heat flux of the IHX between the coupling code and single Locust.

323 Wall temperature	Coupld model	Locust model	323 Heat flux	Coupld model	Locust model
1	518.25	518.06	1	171.95	170.51
2	522.20	522.02	2	184.84	183.57
3	526.45	526.26	3	198.84	197.59
4	531.03	530.82	4	214.04	212.75
5	535.93	535.71	5	230.75	229.58
6	541.22	540.97	6	249.02	247.77
7	546.93	546.65	7	269.01	267.56
8	553.05	552.73	8	291.15	289.59
9	559.68	559.32	9	315.47	313.54
10	566.83	566.40	10	342.25	340.15

TABLE 4. The comparison of the fluid temperature variation along the heat transfer tube of the IHX between the coupling code and single locust.

323P temperature	Coupld model	Locust model	303P temperature	Coupld model	Locust model
1	639.59	639.53	1	500.75	500.73
2	627.26	627.01	2	503.46	503.42
3	615.89	615.48	3	506.37	506.31
4	605.41	604.84	4	509.51	509.43
5	595.72	595.01	5	512.84	512.74
6	586.75	585.93	6	516.43	516.31
7	578.44	577.52	7	520.29	520.16
8	570.73	569.71	8	524.40	524.24
9	563.57	562.51	9	528.85	528.66
10	556.92	555.72	10	533.59	533.38

By comparing the calculated values of the two codes, the state error is within an acceptable range. The maximum deviation of the wall temperature was at the 10th node, and the deviation between the coupled model and the single Locust model was 0.43. Compared with the original value of the single Locust model, the deviation of the coupled model was only 0.076%. The maximum deviation of heat flux was at the first node, and the deviation between coupled model and single Locust model was 2.10. Compared with the original value of 340.15 in single Locust model, the deviation of coupled model was only 0.85%. The maximum deviation of temperature change of 323p was at the 10th node, and the deviation between coupled model and single Locust model was 1.20. Compared with the original value 555.72 of single Locust model, the deviation of coupled model was only 0.22%. The maximum deviation of 303p was at the 10th node, and the deviation between the coupled model and the single Locust model was 0.21. Compared with the original value of 533.38 in the single Locust model, the deviation of the coupled model was only 0.039%. Taking the above

analysis together, the coupled model will not deviate more than 1% from the single Locust model.

B. THE VALIDATION OF TRANSIENT CONDITIONS

Two transient conditions are used to test and verify the rationality of the coupling method. (1) A step decrease of inlet temperature of primary loop from 640K to 630K occurs at 1000s, the testing results are given in Fig.8 (a); (2) A step 10% decrease of LBE flowrate occurs at 1000s, the testing results are shown in Fig.8 (b). When the transient test began at 1000s, the variable curves of nodes of 323P and 303P are similar to the curves of model computed by single Locust.

Table 5 and Table 6 show the comparison of temperature changes of each node under transient conditions. It can be seen that the maximum deviation of the model calculated by the coupled model and the single Locust model is still small in the dynamic process, which indicates that the coupled model also has a good degree of fit under dynamic conditions.In the inlet temperature step change of the primary loop, the maximum deviation of the two models in each node of 323P and 303P was selected for comparison. In the 323P node, the maximum deviation was 0.17, compared with the original value of 594.07 in the single Locust model, the deviation of the coupled model was only 0.029%. In 303P nodes, the maximum deviation is 0.25. Compared with the original value of 528.17 in the single Locust model, the deviation of the coupled model is only 0.047%. In the LBE flowrate step change, the maximum deviation of the two models in each node of 323P and 303P was selected for comparison. In the 323P node, the maximum deviation was 0.25, compared with the original value of 558.67 in the single Locust model, the deviation of the coupled model was only 0.045%. In 303P nodes, the maximum deviation is 0.16, compared with the original value 502.03 of the single Locust model, the deviation of the coupled model is only 0.032%. Therefore, the coupled model will also not deviate more than 1% from the single Locust model in the dynamic process.

Based on the above analysis, it can be seen that the coupling method agrees well with the integrated model under steady and transient conditions, and the error is within an acceptable range (smaller than 1%). This coupling method can be used to establish the ADS simulation model and design the control system.

TABLE 5. The comparison of the fluid temperature variation under A 10k step decrease of LBE inlet temperature.

323P temperature	Maximum deviation point		303P temperature	Maximum deviation point	
	Coupld model	Locust model		Coupld model	Locust model
1	633.51	633.37	2	528.42	528.17
3	617.43	617.28	4	519.56	519.43
5	594.24	594.07	6	513.42	513.31
7	578.61	578.45	8	506.53	506.39
9	563.37	563.24	10	501.47	501.28

TABLE 6. The comparison of the fluid temperature variation under A 10% step decrease of LBE flowrate.

323P temperature	Maximum deviation point		303P temperature	Maximum deviation point	
	Coupld model	Locust model		Coupld model	Locust model
1	639.42	639.34	2	528.39	528.43
3	618.27	618.34	4	521.16	521.04
5	594.38	594.27	6	512.97	512.89
7	579.39	579.25	8	506.72	506.61
9	558.92	558.67	10	502.19	502.03

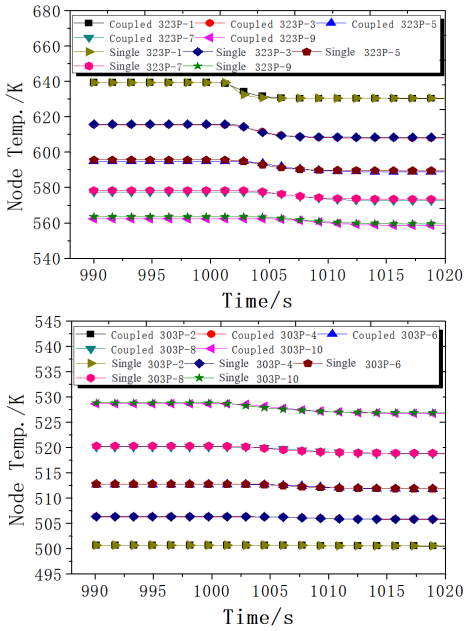

(a) A step decrease of metal reactor inlet temperature

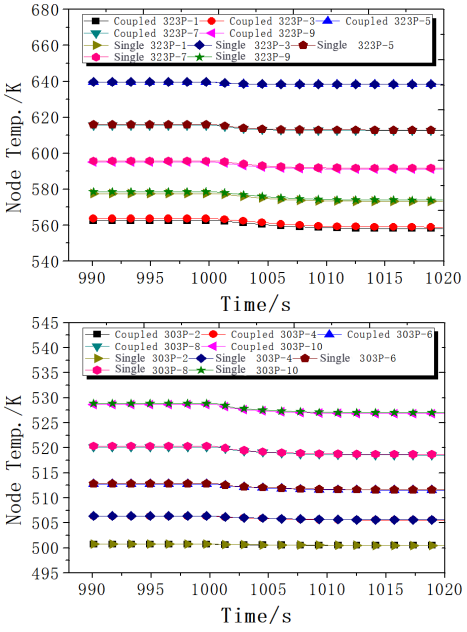

(b) A 10% step decrease of metal reactor flowrate

FIGURE 8. Comparison of transient results between the two codes.

VI. CONTROL SYSTEM SIMULATION AND ANALYSIS

There are two methods of data exchange in this simulation system, the first is the wall temperature and heat flux as data exchange method used to connect modular models of the two codes, the secondary is dynamic data exchange method between thermal-hydraulic(TH) models and control logic. That is to say, control system receives the controlled values of the TH model as input signals include of temperature, pressure, power. etc., and calculates results from control system include valve open degree and fan blowing are sent to the TH model. In this section, the model of the China ADS system and control strategy will be tested and validated in steady and transient conditions.

A. STEADY-STATE VALIDATION

The comparison of the main TH values between this simulation code and the commercial code are used to prove the validity of the coupling and modeling methods in 100% FP and 60%FP conditions. The design data are given by the Locust software, and the precision of main designed values is about 1%.

As shown in Table 7, the steady error is acceptable through comparing the simulation values with design data. Since the steady error of this thermal-hydraulic process variables are inherently determined by the modeling method and the coupling method between loops, the satisfactory steady errors show that the newly-development code with the thermal coupling method is acceptable. Note that this coupling method not only determines the steady states but influences the system transients deeply.

TABLE 7. Steady-state in the 100% FP and 60% FP conditions.

Parameter name	Unit	Parameter Values			
		100%FP		60%FP	
		Design	Simulation	Design	Simulation
Normalized thermal power	MW	1	1.01	0.6	0.66
Core inlet temperature	K	553.15	552.95	553.15	553.35
Core outlet temperature	K	653.15	653.30	614.15	614.40
Secondary side inlet temperature	K	498.15	497.55	498.15	498.60
The PZR pressure	MPa	8	7.95	8	8.05
Air mass flow rate in TC	m^3/s	100	103.5	62	64.5

B. TRANSIENT VALIDATION

The steady-state computational error is acceptable as shown in subsection V. In this subsection, we prove the feasibility of the coupling method and Locust model in different transient conditions. The water flowrate control system and air blow control system are used to keep the main parameters at the reference values.

1.1 Step decrease of power

Supposing the proton beam is linear with power. Initially, the ADS system operates at 100%FP, and at 1500s, a step decrease of power from 100%FP to 90%FP is then induced through changing the proton beam manually. The transient responses of the normalized neutron flux, inlet and outlet coolant temperature of core, inlet coolant temperature of HX, mass flowrate of water and volume flowrate of air are all shown in Fig.9.

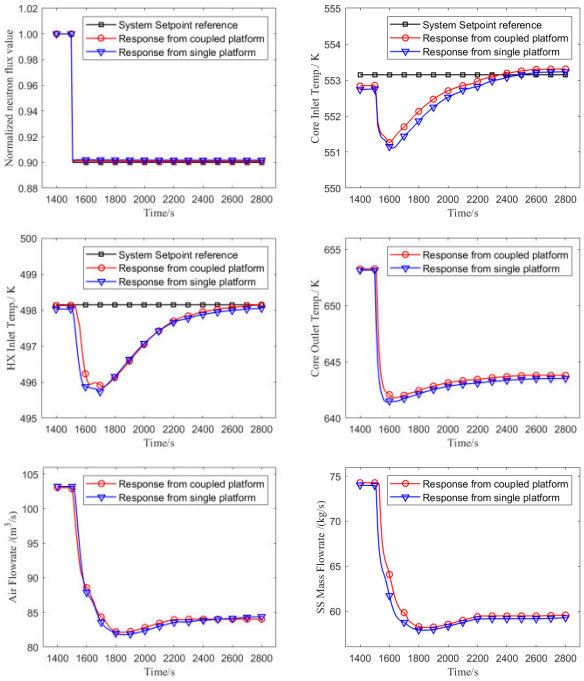

FIGURE 9. Main parameters response to a 10% power demand step decrease.

The step decrease of proton beam causes the prompt decrease of normalized neutron flux, which leads to the decrease in the coolant temperature of primary and secondary loops at the beginning. Then, the core inlet temperature and IHX inlet temperature are well controlled to the objective valves at 2500th second because of the action of control systems. Furthermore, the decrease of LBE average temperature in the IHX weakens the heat transfer from the primary side to the secondary side of IHX, which leads to the decrease of water mass flowrate and air volume flowmate. Then the ADS system finally enters to a new steady state when the powers of different loops are balanced.

Tables 8 and 9 show the overshoot and adjustment time of each thermal hydraulic parameter for the coupled model and the single Locust model under the condition of 10% power reduction, respectively. For practical engineering applications, we require that the overshoot of each control parameter should be less than 5%. The maximum overshoot of the single Locust model is 3.62%, and the maximum overshoot of the

TABLE 8. The Comparison of thermal hydraulic parameters overshoot between the coupling code and single Locust under step decrease of power.

thermal hydraulic parameters	Coupld model	Locust model
normalized neutron flux	/	/
core inlet temperature	0.31%	035%
HX inlet temperature	0.46%	0.52%
core outlet temperature	0.18%	0.21%
air flowrate	2.41%	2.45%
mass flowrate	3.53%	3.62%

TABLE 9. The comparison of thermal hydraulic parameters adjustment time between the coupling code and single Locust under step decrease of power.

thermal hydraulic parameters	Coupld model	Locust model
normalized neutron flux	100.00s	100.00s
core inlet temperature	1134.78s	1131.64s
HX inlet temperature	1157.89s	1162.97s
core outlet temperature	1147.37s	1159.24s
air flowrate	1250.19s	1256.28s
mass flowrate	1159.25s	1162.31s

coupled model is 3.53%, both of which meet the design requirements. At the same time, the maximum adjustment time of the single Locust model is 1256.28s, and the maximum adjustment time of the coupled model is 1250.19s, which both meet the design requirements that the adjustment time should be less than 1500s. We also find that the control indicators of the coupled model and the single Locust model are not much different under the condition of power rise, and the overall effect of the coupled model is slightly better than that of the single Locust model.

1.2 Step increase of power

The ADS system operates at 90%FP initially, and a step increase of proton beam occurs at 1500s. The responses are shown in Fig.10. In this transient condition, the transient variables responses are also well controlled in reasonable range by control systems.

Tables 10 and 11 show the overshoot and adjustment time of each thermal hydraulic parameter for the coupled model and the single Locust model under the condition of 10% power increase, respectively. For practical engineering applications, we require that the overshoot of each control parameter should be less than 5%. The maximum overshoot of the single Locust model is 3.98%, and the maximum overshoot of the coupled model is 3.87%, both of which meet the design requirements. At the same time, the maximum adjustment time of the single Locust model is 1268.27s, and the maximum adjustment time of the coupled model is 1245.63s, which both meet the design requirements that the adjustment time should be less than 1500s. We also find that the control indicators of the coupled model and the single Locust model are not much different under the condition of power rise, and the effect of

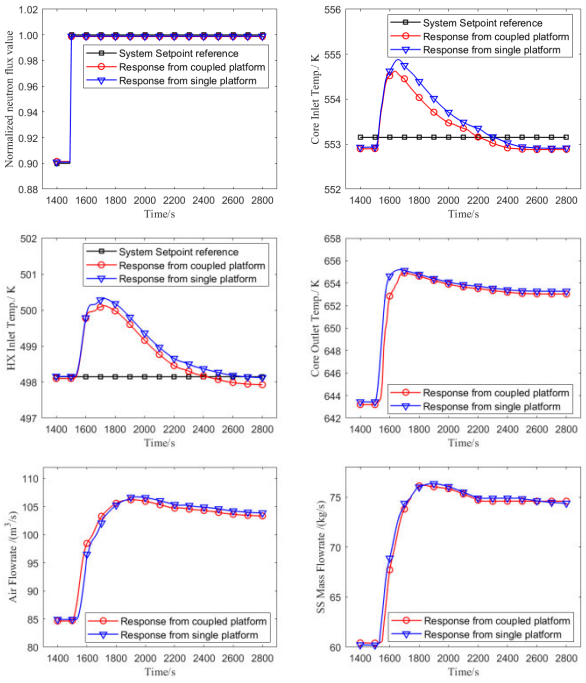

FIGURE 10. Main parameters response to a 10% power demand step increase.

TABLE 10. The comparison of thermal hydraulic parameters overshoot between the coupling code and single Locust under step increase of power.

thermal hydraulic parameters	Coupld model	Locust model
normalized neutron flux	/	/
core inlet temperature	0.24%	0.26%
HX inlet temperature	0.42%	0.44%
core outlet temperature	0.31%	0.32%
air flowrate	3.87%	3.98%
mass flowrate	3.38%	3.52%

TABLE 11. The comparison of thermal hydraulic parameters adjustment time between the coupling code and single Locust under step increase of power.

thermal hydraulic parameters	Coupld model	Locust model
normalized neutron flux	100.00s	100.00s
core inlet temperature	1142.57s	1158.34s
HX inlet temperature	1147.21s	1132.49s
core outlet temperature	1139.23s	1145.60s
air flowrate	1245.63s	1268.27s
mass flowrate	1165.27s	1172.31s

the coupled model is slightly better than the single Locust model.

In summary, the simulation results of power reduction and power increase show that the change curves of the main parameters are consistent with the reality, which further demonstrates the rationality and accuracy of the coupling model, and can meet the simulation requirements for control system design and verification.

VII. CONCLUSION

In this paper, a thermal coupling strategy between Locust and Simulink is proposed, which takes heat flux and wall temperature as interface boundary parameters. To verify the effectiveness of the strategy, OTSG calculated by the coupling model is compared with the thermal hydraulic parameter values calculated by single Locust model under steady and transient conditions. Under steady condition, the maximum deviations of wall temperature, heat flux, temperature change of LBE side and temperature change of water side are 0.076%, 0.85%, 0.22% and 0.039%, respectively. Under the condition of the primary inlet temperature step change, the maximum deviation of the temperature change of the LBE side and the water side of the coupling model is 0.029% and 0.047%, respectively. Under the condition of LBE flow step change, the maximum deviation of temperature change of LBE side and water side of the coupled model is 0.045% and 0.032%, respectively. Simulation results show that the coupled model is in good agreement with the single Locust model. At the same time, based on this platform, the step load variation of 10% FP is simulated to study its control characteristics. Under the condition of 10% power increase, the maximum overshoot and adjustment time of the coupling model are 3.87% and 1245.63s, respectively. Under the condition of 10% power reduction, the maximum overshoot and adjustment time of the coupling model are 3.53% and 1258.19s, respectively. The simulation results show that the control index of the coupled model is slightly better than that of the single Locust model under both increasing power and decreasing power conditions.

Thus, we conclude that the control system has a good ability to regulate the ADS system, which can provide an important reference for further engineering practice. However, according to the work we have completed so far, there are also some improvements that can be made, for example, the control scheme can use more advanced adaptive control, active disturbance rejection control, model predictive control, etc. However, the safety consideration of nuclear power is particularly important, and the advanced control scheme mainly stays at the theoretical research level, and the practical engineering application is difficult. It is the focus of our further work to develop and test an advanced integrated control module that can be applied to new reactor engineering applications such as lead-bismuth fast reactor.

REFERENCES

[1] J.-Y. Li, J.-L. Du, L. Gu, Y.-P. Zhang, C. Lin, Y.-Q. Wang, X.-C. Zhou, and H. Lin, "The optimization study of core power control based on meta-heuristic algorithm for China initiative accelerator driven subcritical system," *Nucl. Eng. Technol.*, vol. 55, no. 2, pp. 452–459, Feb. 2023.

[2] L. L. Salas, F. C. Silva, and A. S. Martinez, "A new point kinetics model for ADS-type reactor using the importance function associated to the fission rate as weight function," *Ann. Nucl. Energy*, vol. 190, Sep. 2023, Art. no. 109869.

[3] K. T. Agbevanu, S. K. Debrah, E. M. Arthur, and E. Shitsi, "Liquid metal cooled fast reactor thermal hydraulic research development: A review," *Heliyon*, vol. 9, no. 6, Jun. 2023, Art. no. e16580.

[4] F. Bianchi, C. Artioli, K. W. Burn, G. Gherardi, S. Monti, L. Mansani, L. Cinotti, D. Struwe, M. Schikorr, W. Maschek, H. A. Abderrahim, D. De Bruyn, and G. Rimpault, "Status and trend of core design activities for heavy metal cooled accelerator driven system," *Energy Convers. Manage.*, vol. 47, no. 17, pp. 2698–2709, Oct. 2006.

[5] L. Cinotti and G. Gherardi, "The Pb–Bi cooled XADS status of development," *J. Nucl. Mater.*, vol. 301, no. 1, pp. 8–14, Feb. 2002.

[6] H. A. Abderrahim, P. Baeten, and D. D. Bruyn, "MYRRHA—A multipurpose fast spectrum research reactor," *Energy Conv. Mang.*, vol. 63, pp. 4–10, Nov. 2012.

[7] R. D. E. Gatchalian and P. V. Tsvetkov, "Reactor physics analysis of a source-driven TRIGA configuration in subcritical domain," *Ann. Nucl. Energy*, vol. 186, Jun. 2023, Art. no. 109787.

[8] C. Reale Hernandez, J. Wallenius, and J. Luxat, "Simulation of a loss of flow transient of a small lead-cooled reactor using a CFD-based model," *Nucl. Eng. Design*, vol. 412, Oct. 2023, Art. no. 112462.

[9] Y. C. Wu, Y. Q. Bai, and Y. Song, "Development strategy and conceptual design of China lead-based research reactor," *Ann. Nucl. Energy*, vol. 87, pp. 516–5111, Jan. 2016.

[10] J.-T. Liu, T.-J. Peng, G. Wang, X.-K. Su, Y.-J. Tao, D.-J. Fan, X.-W. Li, M.-H. He, H.-S. Xu, and L. Gu, "Sub-channel analysis of lead–bismuth fast reactor fuel assembly with wire spacers for China initiative accelerator driven system," *Ann. Nucl. Energy*, vol. 170, Jun. 2022, Art. no. 108965.

[11] R. Zhu, Y. Chen, Y. Lu, X. Wang, and Q. Fu, "Research on structure selection and design of LBE-cooled fast reactor main coolant pump," *Nucl. Eng. Design*, vol. 371, Jan. 2021, Art. no. 110973.

[12] S. Yan, P. Wang, J. Wan, C. Sun, and F. Zhao, "Modeling and controllers design of the China CLEAR-IB," *Nucl. Eng. Design*, vol. 272, pp. 19–27, Jun. 2014.

[13] K. Yin, W. Ma, W. Cui, Z. He, X. Li, S. Dang, F. Yang, Y. Guo, L. Duan, M. Li, and Y. Hou, "Power control of CiADS core with the intensity of the proton beam," *Nucl. Eng. Technol.*, vol. 54, no. 4, pp. 1253–1260, Apr. 2022.

[14] F. Fiori and Z. W. Zhou, "Assessment study of RELAP5/SCDAP capability to reproduce TALL facility thermal hydraulic behavior," *Nucl. Eng. Design*, vol. 295, pp. 15–26, Dec. 2015.

[15] I. Kumari and A. Khanna, "Preliminary validation of RELAP5/Mod4.0 code for LBE cooled NACIE facility," *Nucl. Eng. Design*, vol. 314, pp. 217–226, Apr. 2017.

[16] P. Kakaei, M. Zangian, and M. Abbasi, "Multi-physics core analysis and verification of NuScale reactor with coupling PARCS/RELAP," *Ann. Nucl. Energy*, vol. 193, Dec. 2023, Art. no. 110021.

[17] M. Lin, D. Hou, P. Liu, Z. Yang, and Y. Yang, "Main control system verification and validation of NPP digital I&C system based on engineering simulator," *Nucl. Eng. Design*, vol. 240, no. 7, pp. 1887–1896, Jul. 2010.

[18] A. Toti, J. Vierendeels, and F. Belloni, "Extension and application on a pool-type test facility of a system thermal-hydraulic/CFD coupling method for transient flow analyses," *Nucl. Eng. Design*, vol. 331, pp. 83–96, May 2018.

[19] J.-Y. Li, S.-M. Guo, L. Gu, Y.-P. Zhang, H.-S. Xu, X.-K. Su, and Y.-Q. Wang, "Quantum evolutionary algorithm based power optimization control strategy for China initiative accelerator driven subcritical system," *Ann. Nucl. Energy*, vol. 166, Feb. 2022, Art. no. 108678.

[20] G. Wang, J. Wallenius, R. Yu, W. Jiang, L. Zhang, X. Sheng, D. Yun, and L. Gu, "Transient analyses for China initiative accelerator driven system using the extended BELLA code," *Ann. Nucl. Energy*, vol. 190, Sep. 2023, Art. no. 109892.

[21] Y. Wang, X. Li, X. Huai, J. Cai, and W. Xi, "Experimental investigation of a LBE-helium heat exchanger based the ADS," *Prog. Nucl. Energy*, vol. 99, pp. 11–18, Aug. 2017.

[22] Y. Yang, C. Wang, D. Zhang, S. Qiu, G. Su, and W. Tian, "Heat transfer evaluation of liquid lead-bismuth eutectic cross flow tube bundle: Experimental part," *Int. J. Thermal Sci.*, vol. 193, Nov. 2023, Art. no. 108527.

[23] X. Huang, P. Chen, Y. Yin, B. Pang, Y. Li, X. Gong, and Y. Deng, "Numerical investigation on LBE-water interaction for heavy liquid metal cooled fast reactors," *Nucl. Eng. Design*, vol. 361, May 2020, Art. no. 110567.

[24] S. E. Arda and K. E. Holbert, "A dynamic model of a passively cooled small modular reactor for controller design purposes," *Nucl. Eng. Design*, vol. 289, pp. 218–230, Aug. 2015.

[25] A. J. Humaidi, A. H. Hameed, and M. R. Hameed, "Robust adaptive speed control for DC motor using novel weighted E-modified MRAC," *Proc. IEEE Int. Conf. Power, Control, Signals Instrum. Eng. (ICPCSI)*, 2017, pp. 313–319.

[26] S. M. Mahdi, N. Q. Yousif, A. A. Oglah, M. E. Sadiq, A. J. Humaidi, and A. T. Azar, "Adaptive synergetic motion control for wearable knee-assistive system: A rehabilitation of disabled patients," *Actuators*, vol. 11, no. 7, p. 176, Jun. 2022.
[27] A. Sun, P. Songmao, Z. He, K. Xiao, P. Sun, P. Wang, and X. Wei, "Application of model free active disturbance rejection controller in nuclear reactor power control," *Prog. Nucl. Energy*, vol. 140, Oct. 2021, Art. no. 103907.

TAO ZHANG was born in Nanchong, Sichuan, in 1995. He received the bachelor's degree in measurement and control technology and instrumentation and the master's degree in control engineering from North China Electric Power University, in 2017 and 2022, respectively.

From 2017 to 2019, he was engaged in thermal control maintenance work with Sichuan Bema CFB Demonstration Power Station. From 2019 to 2021, he worked on smart energy with the China National Nuclear Power Planning and Design Institute. Since 2022, he has been an Engineer with China Nuclear Power Technology Research Institute Company Ltd. His current research interests include the design of new reactor control systems and the engineering application of advanced control technology.

Mr. Zhang was a member of the Chinese Society of Electrical Engineering and the Chinese Nuclear Society, in 2022. He has won the National Energy Group Five Small Achievement Award and the First Prize in the National Computer Skills Competition.

BO SHI was born in Qiqihar, Heilongjiang, in 1987. He received the bachelor's and master's degrees in nuclear science and technology from Harbin Engineering University, in 2012 and 2015, respectively.

Since 2015, he has been a Senior Engineer with China Nuclear Power Technology Research Institute Company Ltd. His current research interests include the development of new reactors and the design and verification of control systems.

Mr. Shi was a member of the Chinese Society of Electrical Engineering and the Chinese Nuclear Society, in 2017. He has won the CGNPC Outstanding Contribution Award and the Excellent Paper Award.

ZHIJIANG WU was born in Henan, China. He received the B.Eng. degree from Shandong University, Jinan, China, in 2022, with a focus on the practical application of automation technology in the industrial field.

He is currently an Assistant Engineer with China Nuclear Power Technology Research Institute Company Ltd. His current research interest includes the design of nuclear reactor control systems.

TIANJIAO ZHANG was born in Linfen, China, in 1998. She received the bachelor's degree in mechatronic engineering from Shanxi University, China, in 2020, and the master's degree in control science and engineering from Northeastern University, China, in 2023.

Since 2023, she has been an Engineer with China Nuclear Power Technology Research Institute Company Ltd. Her current research interests include optimal design and operation control for nuclear power generation systems.

YAN WANG was born in Xiangyang, China. She received the M.Eng. degree in control science and engineering from the Guangdong University of Technology, Guangzhou, China, in 2023. She is currently with China Nuclear Power Technology Research Institute Company Ltd. Her current research interests include liquid level control in steam generators and intelligent control.

WEI GUO received the bachelor's degree in nuclear engineering and technology and the master's degree in nuclear technology and application from the Chengdu University of Technology, in 2005 and 2008, respectively. He is currently pursuing the Ph.D. degree in power and energy from Harbin Engineering University.

Since 2008, he has been engaged in the research and development of new reactors and the optimization of control systems with China Nuclear Power Technology Research Institute Company Ltd. He was a Senior Engineer with the China General Nuclear Power Group, in 2022. He has more than ten issued/pending patents. His current research interests include the optimal design and operation control of nuclear power control systems. He has won more than 30 national, provincial, and ministerial-level science and technology awards.